

Detecting Adversarial Faces Using Only Real Face Self-Perturbations

Qian Wang¹, Yongqin Xian², Hefei Ling^{1,*}, Jinyuan Zhang³,
Xiaorui Lin³, Ping Li¹, Jiazhong Chen¹, Ning Yu⁴

¹Huazhong University of Science and Technology, Wuhan, China

²Google, Switzerland

³Software Development Center, Industrial and Commercial Bank of China

⁴Salesforce Research, USA

¹{yqwq1996, lhefei, lpshome, jzchen}@hust.edu.cn, ²yxian@google.com,

³{zhangjy, linxr}@sdc.icbc.com.cn, ⁴ning.yu@salesforce.com

Abstract

Adversarial attacks aim to disturb the functionality of a target system by adding specific noise to the input samples, bringing potential threats to security and robustness when applied to facial recognition systems. Although existing defense techniques achieve high accuracy in detecting some specific adversarial faces (adv-faces), new attack methods especially GAN-based attacks with completely different noise patterns circumvent them and reach a higher attack success rate. Even worse, existing techniques require attack data before implementing the defense, making it impractical to defend newly emerging attacks that are unseen to defenders. In this paper, we investigate the intrinsic generality of adv-faces and propose to generate pseudo adv-faces by perturbing real faces with three heuristically designed noise patterns. We are the first to train an adv-face detector using only real faces and their self-perturbations, agnostic to victim facial recognition systems, and agnostic to unseen attacks. By regarding adv-faces as out-of-distribution data, we then naturally introduce a novel cascaded system for adv-face detection, which consists of training data self-perturbations, decision boundary regularization, and a max-pooling-based binary classifier focusing on abnormal local color aberrations. Experiments conducted on LFW and CelebA-HQ datasets with eight gradient-based and two GAN-based attacks validate that our method generalizes to a variety of unseen adversarial attacks.¹

1 Introduction

Deep neural networks have been widely used in many tasks [Ou *et al.*, 2017; Shi *et al.*, 2020; Zhang *et al.*, 2021], and have achieved remarkable success in facial recognition systems (FRS) [Deng *et al.*, 2019] with a wide range of real-world applications such as online payment [Avarikioti *et al.*, 2019] and financial management [Dumbre *et al.*,

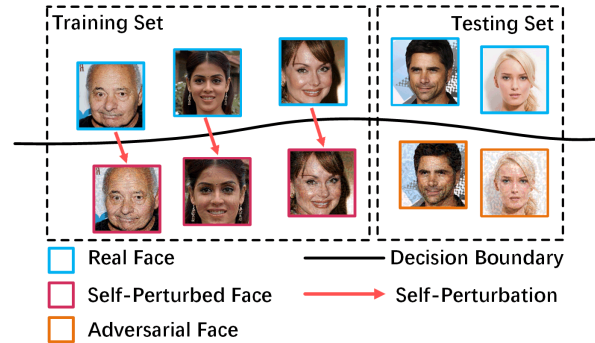


Figure 1: Trained only on real faces and their self-perturbed faces, the detector learns a generic representation of adversarial faces produced by unseen attacks.

[2016]. However, deep neural networks are known to be vulnerable to adversarial attacks [Goodfellow *et al.*, 2014; Kurakin *et al.*, 2016; Madry *et al.*, 2017], making commercial FRSs unreliable.

Some research attempts to defend against adversarial attacks by adversarial example detection techniques [Feinman *et al.*, 2017; Ma *et al.*, 2018; Tian *et al.*, 2021] which filter out adversarial samples before feeding them into protected systems. However, they tend to overfit to known attacks and do not generalize well to unseen advanced attacks [Wu *et al.*, 2021; Yang *et al.*, 2021]. In specific, GAN-based adversarial attacks such as AdvMakeup [Yin *et al.*, 2021] and AMT-GAN [Hu *et al.*, 2022] are recently developed to generate more natural adversarial faces (adv-faces) by adding completely different noise patterns to face images in contrast to traditional gradient-based attacks such as FGSM [Goodfellow *et al.*, 2014], and are able to circumvent detection. Therefore, a plug-and-play method of detecting adv-faces with improved generalization performance over both unseen gradient-based attacks and unseen GAN-based attacks is highly demanded.

Due to the insight that adversarial samples are all modified from real samples [Ma *et al.*, 2018], one direct way to encourage models to learn generic representations for detecting adv-faces is to train models with synthetic data [Shiohara and Yamasaki, 2022], forming a decision boundary wrapping the synthetic subspace. To achieve this, we investigate the intrinsic generality of adv-faces generated by gradient-based

*Corresponding author

¹Code at <https://github.com/cc13qq/SAPD>

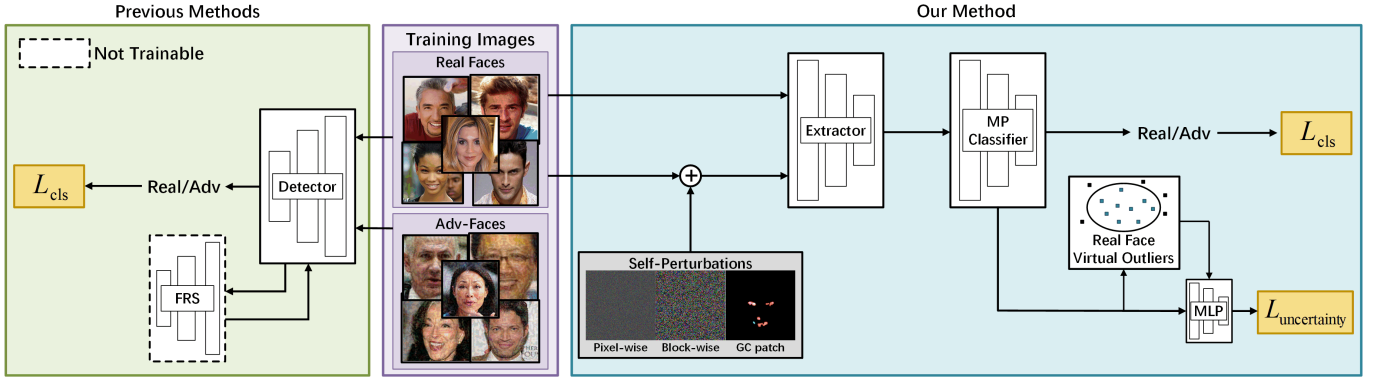


Figure 2: Overview of training pipeline. We design three kinds of self-perturbations to generate synthesized pseudo-adv faces. "GC patch" denotes a gradient color patch for GAN-based attack. "MP Classifier" denotes Max-Pooling Classifier which focuses on abnormal local color aberrations. By synthesizing virtual outliers of real faces, we incorporate an uncertainty loss to regularize the decision boundary to enhance detection performance on adv-faces. Previous methods require pre-computed adv-faces and access permission to the victim FRS for training. By contrast, our method is agnostic to both attacks and FRS. Using only real faces with self-perturbations in the training phase, our method is able to detect all kinds of adv-faces from unseen attacks without modifying or visiting FRS.

attacks and GAN-based attacks respectively, and propose two assumptions: (1) Gradient-based attacks have a resemblance in noise pattern on account of the consistency of the basic attack algorithm which uses gradients to construct adversarial examples. (2) GAN-based attacks aim to simultaneously change the prediction of FRSs while preserving visual quality. In the meantime, FRSs pay the most attention to high-frequency regions [Li *et al.*, 2020], which induces GANs to modify these regions. Therefore, GAN-made adv-faces have manipulated clues like abnormal color aberrations in high-frequency regions. If universal noise patterns that cover all kinds of adversarial noises are attainable, a set of pseudo adv-faces could be produced, and we can train a model with them to learn generic representations for adv-faces.

Based on the above assumptions, we propose three kinds of real face self-perturbations synthesized with pseudo noise patterns which summarize adversarial noises of gradient-based attacks and GAN-based attacks, and a max-pooling-based classifier focusing on capturing abnormal local color aberration. Unlike previous methods, this data-augmentation-like method is proposed from a novel and more intrinsic perspective by investigating the generality of adversarial noise patterns, to detect all recent adv-faces from unseen attacks, protecting FRSs without access to them. Trained on only real faces and their self-perturbations, as shown in Figure 1, our model is able to detect all the recent adv-faces. This new framework simultaneously ensures detection performance on unseen adversarial attacks and portability in use, without any access to protected systems.

Although we are trying to make self-perturbed faces as general as possible, the trained network still overfits to in-domain data and might fail to classify adv-faces far away from the distribution of self-perturbed faces. Regarding adv-faces as out-of-distribution (OOD) data from a shifted data manifold [Deng *et al.*, 2021], we incorporate a regularization term to narrow the model's decision boundary of real face class during training, and naturally introduce a novel cascaded system for adv-face detection, which consists of training data self-perturbations, decision boundary regularization,

and max-pooling-based binary classifier. We evaluate our approach on LFW and CelebA-HQ datasets with eight gradient-based attack methods and two GAN-based attack models. Experiment results validate our assumptions and demonstrate the reliability of our detection performance on adv-faces from unseen adversarial attack methods.

Our contributions are summarized in four thrusts:

- By investigating the intrinsic similarities among varying adv-faces, we propose two assumptions that (1) different adversarial noises have resemblances, and (2) color aberrations exist in high-frequency regions. We empirically validate the assumptions which in turn indicate universal noise patterns are attainable for all the recent adv-faces.
- Based on our assumptions, we propose three kinds of real face self-perturbations for gradient-based adv-faces and GAN-based adv-faces. We are the first to train an adv-face detector using only real faces and their self-perturbations, agnostic to victim FRSs and agnostic to adv-faces. This enables us to learn generalizable representations of adv-faces without overfitting to any specific one.
- We then naturally introduce a novel cascaded system for adv-face detection, which consists of training data self-perturbations, decision boundary regularization, and a max-pooling-based binary classifier focusing on abnormal local color aberrations.
- Evaluations are conducted on LFW and CelebA-HQ datasets with eight gradient-based attacks and two GAN-based attacks, demonstrating the consistently improved performance of our system on adv-face detection.

2 Related Work

Adversarial attacks Adversarial attacks [Goodfellow *et al.*, 2014] aim to disturb a target system by adding subtle noise to input samples, while maintaining imperceptibility from human eyes. In contrast to previous works [Madry *et al.*, 2017; Kurakin *et al.*, 2016], DIM [Wu *et al.*, 2021] and TIM [Dong *et al.*, 2019] are improved attack algorithms with enhanced black-box attack accuracy and breaching several defense techniques. Focusing on breaking

through FRSs, TIPIM [Yang *et al.*, 2021] generates adversarial masks for faces to conduct targeting attacks while remaining visually identical to the original version for human beings. Recently, GAN-based attack models [Yin *et al.*, 2021; Hu *et al.*, 2022] are presented to generate adversarial patches and imperceptible adv-faces, bringing new challenges to adv-faces detection. In this paper, we proposed a simple yet effective detection method against all the above attacks while being blind to them during training.

Adversarial example detection One of the technical solutions for protecting DNNs from adversarial attacks is adversarial example detection [Feinman *et al.*, 2017], aiming to filter out adversarial inputs before the protected system functions. Remedying the limitations of the previous method, LID [Ma *et al.*, 2018] is proposed for evaluating the proximity of an input to the manifold of normal examples. Incorporated with wavelet transform, SID [Tian *et al.*, 2021] is able to transform the decision boundary and can be collaboratively used with other classifiers. While all of these methods focus on utilizing features subtracted by FRS backbone and show effective performance in detecting adversarial examples, they require modifying or visiting the protected system and do not generalize well to new-type attacks like GAN-based AMT-GAN [Hu *et al.*, 2022] and AdvMakeup [Yin *et al.*, 2021]. To address the problems above, our method is proposed to detect all recent adv-faces from unseen attacks, protecting FRSs without access to them.

Out-of-distribution (OOD) detection OOD detection techniques [Girish *et al.*, 2021] have been widely used in image classification tasks [Yu *et al.*, 2019], trying to recognize examples from an unknown distribution. ODIN [Liang *et al.*, 2017] uses temperature scaling and tiny perturbations to the inputs to separate the in-distribution (ID) and OOD images. Lee *et al.* [Lee *et al.*, 2018] uses the Mahalanobis distance to evaluate the dissimilarity between ID and OOD samples. By sampling and synthesizing virtual outliers from the low-likelihood regions, VOS [Du *et al.*, 2022] adaptively regularizes the decision boundary during training. Sun *et al.* [Sun *et al.*, 2021] introduce a simple and effective post hoc OOD detection approach utilizing activation truncation. Regarding adv-faces as OOD data, we leverage an uncertainty regularization term to narrow the decision boundary of real face class during the training phase to boost the accuracy of adv-faces detection.

3 Methodology

We propose a plug-and-play cascaded system for adv-faces detection method which consists of training data self-perturbations, decision boundary regularization, and a max-pooling-based binary classifier focusing on abnormal local color aberrations, agnostic to unseen adversarial attacks, and agnostic to victim FRSs. Training pipeline as shown in Figure 2. We propose to synthesize diverse self-perturbed faces by adding three noise patterns to real face images, summarizing adv-faces generated from gradient-based and GAN-based attacks. A convolutional neural network is learned via real faces and self-perturbed faces, regularized by uncertainty loss, to distinguish real and adversarial faces. As no attack

Algorithm 1 Self-perturbation for gradient-based attack

Input: A empty perturbation matrix $\eta^p \in \mathbb{R}^{H \times W \times 3}$ with the same shape of real face image \mathbf{x}^r .

Parameter: Max perturbation magnitude ϵ , pattern mode.

Output: Self-perturbed face image \mathbf{x}^p .

```

1: A random direction matrix  $R = \{\vec{r}_{ij}\} \in \mathbb{R}^{H \times W \times 3}$ .
2: for  $\vec{\eta}_{ij}$  in  $\eta^p$  do
3:   Select random noise value  $\alpha$ .
4:   if pattern mode is ‘point-wise’ then
5:      $\vec{\eta}_{ij} := \alpha \cdot \vec{r}_{ij}$ .
6:   else if pattern mode is ‘block-wise’ then
7:     Select a random neighborhood  $A_{ij}$  of  $\vec{\eta}_{ij}$ .
8:     for  $\vec{\eta}_{ijk}$  in  $A_{ij}$  do
9:        $\vec{\eta}_{ijk} := \alpha \cdot \vec{r}_{ij}$ .
10:    end for
11:   end if
12: end for
13: Clip perturbation  $\eta^p$  using Equation 2.
14: Generate self-perturbed face  $\mathbf{x}^p$  using Equation 3.
15: return  $\mathbf{x}^p$ 

```

method is observed during training, the resulting network is not biased to any attack, yielding generic and discriminative representations for detecting unseen adv-faces. Therefore, in the testing phase, the embeddings are sent to the learned Max-Pooling Classifier to accomplish prediction.

3.1 Real Face Self-Perturbations

Self-perturbation for gradient-based attack Given a real face image \mathbf{x}^r , adversarial attack generates an adversarial image \mathbf{x}^a by adding a perturbation image η to \mathbf{x}^r [Goodfellow *et al.*, 2014]:

$$\mathbf{x}^a = \mathbf{x}^r + \eta, \quad (1)$$

where $\|\eta\| \leq \epsilon$, and ϵ called perturbation magnitude.

We observe that a binary classifier trained on real faces and adv-faces generated by FGSM is able to classify a part of attack images generated from other attack methods as shown in Table 2. This generalization in classification means that attack noises have intrinsic similarities. And it means once we master all the similarities we master the attacks, even for unseen attacks. This leads to non-trivial designs for our self-perturbation image η^p .

The noise value of neighbor points in η^p may be the same or different. From this perspective, we introduce point-wise and block-wise noise patterns for gradient-based attacks. As presented in Algorithm 1, we perturb each point in the point-wise pattern and each block in the block-wise pattern in a stochastic direction, where blocks are random neighborhoods of a set of scattered points. The generated perturbation image η^p is constrained in l^∞ norm, and clipped according to ϵ ,

$$\eta^p = \text{Clip}_{[-\epsilon, \epsilon]}(\eta^p). \quad (2)$$

And self-perturbed face is calculated as

$$\mathbf{x}^p = \mathbf{x}^r + \eta^p. \quad (3)$$

Algorithm 2 Self-perturbation for GAN-based attack

Input: Real face image \mathbf{x}^r . A empty perturbation matrix $\eta^p = \{\eta_{ij}\}$ with the same shape of \mathbf{x}^r .

Parameter: Max perturbation magnitude ϵ , face landmarks, high-frequency threshold γ , and empty high-frequency pixel set H .

Output: Self-perturbed face image \mathbf{x}^p .

Function: $\text{value}(x)$ measures pixel value of x , $\text{neighborhood}(x)$ is a random neighborhood of x .

- 1: Obtain gradient image of \mathbf{x}^r using Sobel operator.
 - 2: Obtain high-frequency convex hull from gradient image according to landmarks.
 - 3: **for** x_{ij} **in** convex hull **do**
 - 4: **if** $\text{value}(x_{ij}) < \gamma$ **then**
 - 5: η_{ij} join to H .
 - 6: **end if**
 - 7: **end for**
 - 8: Random select a subset H_s of H .
 - 9: **for** η_{ij}^H **in** H_s **do**
 - 10: Generate a random gradient color patch P .
 - 11: $\text{neighborhood}(\eta_{ij}^H) := P$.
 - 12: **end for**
 - 13: Clip perturbation η^p using Equation 2.
 - 14: Generate self-perturbed face \mathbf{x}^p using Equation 3.
 - 15: **return** \mathbf{x}^p
-

Self-perturbation for GAN-based attack Spectrums of real and fake images distribute differently in high frequency [Luo et al., 2021], such as eyes, nose, and mouth. This distribution difference should become more intense because GAN-made adv-faces aim to change the classification results of FRSS meanwhile maintain perceptual invariance. This leads to color aberration and boundary abnormality in high-frequency regions on account of that FRSS pay the most attention to these regions. Focusing on producing natural and imperceptible attack noise, these abnormal color aberrations should have gradient or blurred boundaries. In such a perspective, we use gradient color patches to act as self-perturbation.

As presented in Algorithm 2, we first obtain the gradient image of a real image using Sobel operator [Duda and Hart, 1973] and convex hull of the high-frequency area according to facial landmarks. The pixels in the convex hull are selected as high-frequency pixels if their values surpass a threshold γ . Then we generate a few gradient color patches through a series of affine transformations. Finally, the pseudo adv-faces are generated by adding gradient color patches to a random set of high-frequency pixels.

After crafting a part of real faces to self-perturbed faces as negative samples, we label other real faces as positive samples and train a well-designed backbone network such as XceptionNet [Chollet, 2017] in a binary classification manner.

3.2 Max-Pooling Classifier

In view of abnormal speckles in GAN-based adv-faces are always tiny and are not easy to be observed, we proposed Max-Pooling Classifier (MPC) to capture abnormal local color

aberrations. MPC produces classification scores and predicts whether input images are real or adversarial.

A typical backbone network includes a feature extractor $f(\cdot; \varphi)$ composed of several convolutional blocks, and a classifier $g(\cdot; \phi)$ comprising an average pooling layer, an activation layer, and a fully connected layer [Chollet, 2017]. To detect adv-faces with abnormal local color aberrations, a simple derivation is to divide an image into several rectangle areas, and if abnormal color aberration occurs in any of the rectangle areas we classify this image as adv-face.

Input an image \mathbf{x} to feature extractor $f(\cdot; \varphi)$, it produces a feature map $M(\mathbf{x}) \in \mathbb{R}^{N \times N \times d}$ composed of $N \times N$ features, where d is the embedding size, and each feature is corresponding to a rectangle area i.e. the receptive field. Features are sent to the activation function and fully connected layer respectively and produce $N \times N$ logits. We take the max-pooling of these logits as the final logit and obtain prediction score $S_{\text{cls}} \in \mathbb{R}^2$ by softmax operation. Classification of input image \mathbf{x} is computed by argmax function:

$$G_{\text{cls}}(\mathbf{x}) = \text{argmax}(S_{\text{cls}}), \quad (4)$$

where $G_{\text{cls}}(\mathbf{x}) = 1$ indicates real face and $G_{\text{cls}}(\mathbf{x}) = 0$ indicates adv-face.

3.3 Decision Boundary Regularization

Although we are trying to make self-perturbed faces as general as possible, the trained network still overfits to ID data and might fail to classify faces far away from the distribution of negative samples. Regarding adv-faces as OOD data, we incorporate a regularization term [Du et al., 2022] to our work to enhance adv-face detection performance.

Assuming the feature representation of real faces forms a multivariate Gaussian distribution, we sample virtual outliers $\mathcal{V} \subset \mathbb{R}^m$ from the ϵ -likelihood region of the estimated class-conditional distribution:

$$\mathcal{V} = \left\{ \mathbf{v} \mid \frac{\exp\left(-\frac{1}{2}(\mathbf{v} - \hat{\boldsymbol{\mu}})^\top \hat{\boldsymbol{\Sigma}}^{-1}(\mathbf{v} - \hat{\boldsymbol{\mu}})\right)}{(2\pi)^{m/2} |\hat{\boldsymbol{\Sigma}}|^{1/2}} < \epsilon \right\}, \quad (5)$$

where $\hat{\boldsymbol{\mu}}$ and $\hat{\boldsymbol{\Sigma}}$ are the estimated mean and covariance using latent features of real faces.

The uncertainty loss regularizes the model to produce a low OOD score for ID data and a high OOD score for the synthesized outliers, and narrows the decision boundary of real face class to boost the performance of adv-face detection:

$$\begin{aligned} \mathcal{L}_{\text{uncertainty}} = & \mathbb{E}_{\mathbf{v} \sim \mathcal{V}} \left[\log(\exp^{-\phi(-f(\mathbf{v}; \theta))} + 1) \right] \\ & + \mathbb{E}_{\mathbf{x} \sim \mathcal{D}^r} \left[\log\left(\frac{1}{\exp^{-\phi(-f(\mathbf{x}; \theta))} + 1}\right) \right], \end{aligned} \quad (6)$$

where \mathcal{D}^r represents distribution of real face, $f(\cdot; \theta)$ is a linear transformation function, and $\phi(\cdot)$ is a nonlinear MLP function. The learning process shapes the uncertainty surface, which predicts a high probability for ID data and a low probability for virtual outliers \mathbf{v} .

The training objective combines the real-adv classification loss and the regularization term:

$$\min_{(\mathbf{x}, y) \sim \mathcal{D}} (\mathcal{L}_{\text{cls}} + \beta \cdot \mathcal{L}_{\text{uncertainty}}), \quad (7)$$

	Study	Method	Detect Attacks	Attack-Agnostic	FRS-Agnostic
AD	LID [Ma et al., 2018]	Local intrinsic dimensionality	Gradient-based	×	×
	SID [Tian et al., 2021]	Wavelet transform	Gradient-based	×	×
FD	Luo et al. [Luo et al., 2021]	SRM convolution + DCMA	GAN-based	×	✓
	He et al. [He et al., 2021]	Re-Synthesis Residuals	GAN-based	×	✓
OOD	ODIN [Liang et al., 2017]	Softmax score	Gradient-based + GAN-based	✓	×
	MD [Lee et al., 2018]	Mahalanobis distance.	Gradient-based + GAN-based	✓	×
	ReAct [Sun et al., 2021]	Rectified truncation	Gradient-based + GAN-based	✓	×
	Ours	Self-Perturbation	Gradient-based + GAN-based	✓	✓

Table 1: Baselines used in our study. "AD" and "FD" denotes adversarial example detection and face forgery detection respectively. "OOD" denotes OOD detection. "Attack-Agnostic" means that attacks are unseen and no adv-faces are required for training. "FRS-Agnostic" means that victim FRS are unknown and access is forbidden. Only our method does not rely on pre-computed adv-faces or victim FRS.

where \mathcal{D} represents the distribution of training data. β is the weight of the regularization $\mathcal{L}_{\text{uncertainty}}$, and \mathcal{L}_{cls} is the Cross-Entropy classification loss [Zhang and Sabuncu, 2018].

4 Experiment

To validate the detection performance of our approach on adv-faces generated by various adversarial attack methods, we conduct extensive empirical studies on two datasets in this section. We validate our assumptions by investigating the intrinsic similarity of adv-faces and compare our method to baselines from three research streams. After that, we analyze our approach through a series of ablation studies.

General setup During model training, real faces are used as positive samples, and only self-perturbations of real faces are used as negative samples. Any adv-faces are agnostic. During testing, all the negative samples are adv-faces. In detail, half of the real faces in the training phase are labeled 1 as the positive samples, and others are self-perturbed and labeled 0 as the negative samples. In the testing phase, all of adv-faces are labeled 0. For evaluating the performance of detectors, we choose the widely used AUC score as the main metric.

Datasets Face images in this work are sampled from LFW [Gary et al., 2007] and CelebA-HQ [Karras et al., 2017] datasets. LFW contains 13,233 face images of 5,749 subjects. Subjects with at least two face images take part in adv-face producing. The first image of each subject is regarded as a reference and the others are sampled to produce adv-faces which includes 7,484 images. CelebA-HQ is a high-resolution subset of CelebA, containing 30,000 images.

Attack methods We employ eight recent gradient-based adversarial attack methods FGSM [Goodfellow et al., 2014], BIM [Kurakin et al., 2016], PGD [Madry et al., 2017], RFGSM [Tramèr et al., 2018], MIM [Dong et al., 2018], DIM [Wu et al., 2021], TIM [Dong et al., 2019] and TIPIM [Yang et al., 2021], and two GAN-based attack methods: AdvMakeup [Yin et al., 2021] and AMT-GAN [Hu et al., 2022] as attackers, and ArcFace [Deng et al., 2019] as victim FRS to produce adv-faces on gradient-based attacks. All the gradient-based attacks are applied on LFW and CelebA-HQ datasets to generate adv-faces, while AdvMakeup and AMT-GAN are on the CelebA-HQ dataset.

Detector	FGSM	PGD	DIM	TIM	AdvM.
FGSM	100	99.9	99.7	49.2	0.0
PGD	99.4	100	99.7	6.8	0.0
DIM	98.7	99.4	99.6	2.2	0.0
TIM	71.3	85.8	79.5	93.2	0.0
AdvM.	22.1	19.9	19.5	23.2	98.5

Table 2: Detection accuracy (%) on adv-faces generated by various of attack algorithms. All adv-faces are generated at $\epsilon = 5/255$. Networks are trained on adv-faces generated by attacks in the left column, and tested on adv-faces produced by attacks in the top row.

Implementation details We modify an ImageNet-pre-trained XceptionNet [Deng et al., 2009; Chollet, 2017] as the backbone network in our method. We set $N = 7$ to produce a 7×7 feature map in the last convolution layer and choose ReLU as an activation function. We utilize DLIB [Sagonas et al., 2016] for face extraction and alignment, Torchattacks [Kim, 2020] for generating adv-faces, and OpenOOD [Girish et al., 2021] for network training. All face images are aligned and resized to 256×256 before training and testing. The perturbation magnitude ϵ in self-perturbations and adv-faces producing is set to $5/255$, a small value. Threshold γ in the convex hull of gradient image in Algorithm 2 is set to 50. The regularization loss weight β is set to 0.1. Training epochs are set to 5 and convergence is witnessed.

Baselines Previous adversarial example detection methods [Ma et al., 2018; Tian et al., 2021] focus on specific tasks or gradient-based attacks and hence can hardly be effectively extended to GAN-based adv-faces, while face forgery detection methods [Luo et al., 2021; He et al., 2021] are used to detect GAN-made fake faces. On the other hand, some OOD detection methods [Liang et al., 2017; Lee et al., 2018; Sun et al., 2021] only rely on output features and logits of the backbone network and keep agnosticism to unknown attacks, closing to our setting. On account of this, we compare our method to various methods in three problem settings. All baselines listed in Table 1 include methods of adversarial example detection, OOD detection, and face forgery detection. It is worth noting that only our method does not require either pre-computed adv-faces or access to FRS.

4.1 Assumption Validation

Our assumption for gradient-based noise patterns stands on the visual similarities between adversarial noises. However,

Method	LFW								CelebA-HQ							
	FGSM	BIM	PGD	RF.	MIM	DIM	TIM	TIP.	FGSM	BIM	PGD	RF.	MIM	DIM	TIM	TIP.
LID	76.7	74.0	70.7	73.0	77.7	70.2	62.1	69.0	82.0	55.2	52.5	54.4	57.7	53.7	54.0	59.3
SID	99.7	81.8	73.7	77.8	90.1	72.2	73.4	88.5	96.7	79.2	63.4	72.8	84.5	76.4	81.0	85.2
ODIN	75.6	71.1	71.6	75.2	79.8	73.6	74.8	71.4	76.7	75.7	75.8	75.7	75.0	76.0	72.4	72.2
MD	95.2	91.3	91.9	91.4	90.1	94.0	88.9	86.6	94.1	91.6	91.6	91.7	90.7	93.2	91.9	87.4
ReAct	92.3	89.2	88.4	89.1	89.9	92.2	91.3	90.8	93.6	90.7	90.5	90.6	89.9	92.3	91.9	87.3
Ours	100	100	100	100	99.9	99.7	100	100	99.7	99.0	99.6	99.4	98.1	99.5	96.2	91.7

Table 3: Comparison of AUC scores (%) of detecting gradient-based adv-faces from LFW and CelebA-HQ datasets. Detectors of LID and SID are trained on FGSM adv-faces. As for other detectors, all attacks are unseen. "RF." denotes RFGSM and "TIP." denotes TIPIM.

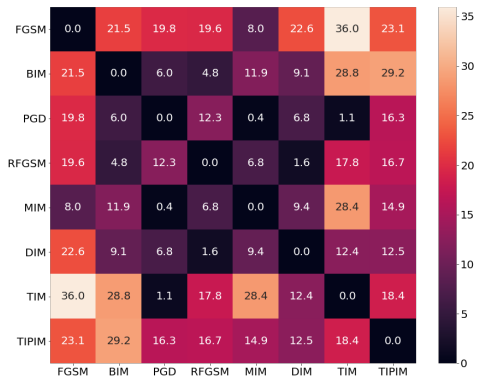


Figure 3: Fréchet Inception Distance heat map of various attacks.

the human eye is sometimes unreliable because we cannot observe tiny differences between pixels. To verify the reliability of the hypotheses, we train a simple XceptionNet with real faces from the CelebA-HQ dataset and adv-faces generated by one attack algorithm and test detection accuracy on 1,000 adv-faces per attack. As shown in Table 2, a detector for a specific gradient-based attack is able to generalize to other attacks except those based on GANs. but the success rate on some attacks such as TIM is much lower. We also calculate the Fréchet Inception Distance of various attacks in Figure 3 to visualize distribution similarity. What the results demonstrate is that attack noises are to some extent similar to each other, and the way of extracting a universal noise pattern is feasible. The result also indicates that noise patterns of GAN-based attacks are not close to gradient-based attack noise patterns and need to be specifically treated.

4.2 Main Results

Gradient-based adv-face detection We first compare the detection performance of our method to other detectors on gradient-based attacks. Baselines include 2 detectors proposed for adversarial example detection [Ma *et al.*, 2018; Tian *et al.*, 2021] and 3 detectors for OOD detection [Liang *et al.*, 2017; Lee *et al.*, 2018; Sun *et al.*, 2021]. The detectors are trained on real images, along with adv-faces images (LID and SID) or pseudo adv-faces images (Ours). We compute the classification AUC for all methods on a dataset comprising of 1k real images and 1k adversarial face images per attack type in LFW and CelebA-HQ datasets.

As shown in Table 3, trained on the known attack (FGSM), previous adversarial example detection methods is difficult to detect unknown attacks. In a contrast, our method reaches a high level of detecting gradient-based adv-faces and almost

Method	Adv-Makeup	AMT-GAN	Mean
He et al.	52.5	88.2	70.4
Luo et al.	61.8	65.1	62.0
ODIN	63.3	69.7	66.5
MD	72.3	78.2	72.3
React	77.6	82.9	80.3
Ours	96.6	89.7	93.2

Table 4: Comparison of AUC (%) of detecting GAN-based adv-faces from CelebA-HQ dataset. All attacks are unseen by all detectors. The detector of He et al. is pre-trained on CelebA-HQ and detector of Luo et al. is pre-trained on FF++ [Rössler *et al.*, 2019].

approaches saturation performance on the LFW dataset. This is likely because the network learns a generic representation for adv-faces. The result that the AUC score on LFW is higher than which on CelebA-HQ may contribute to the fact that CelebA-HQ is a more complicated dataset with high resolution and diversified background so self-perturbation works much harder on it. Thus we speculate that a more complex and more diversified data environment will increase the difficulty of adv-face detection tasks.

GAN-based adv-face detection To investigate the advantage of our method on detecting GAN-based samples, we make comparisons with SOTA methods of face forgery detection [He *et al.*, 2021; Luo *et al.*, 2021] and OOD detection [Liang *et al.*, 2017; Lee *et al.*, 2018; Sun *et al.*, 2021]. We train our model with only real faces and self-perturbed faces from CelebA-HQ and test both our approaches and baseline models on GAN-based adv-faces. As shown in Table 4, the performance of our method exceeds which of other algorithms and models. This result verifies our assumption that GAN-made adv-faces have manipulated clues like an abnormal color aberration in high-frequency regions. The observation that detection performance on Adv-Makeup is higher than which on AMT-GAN is likely because abnormal local aberrations of Adv-Makeup are more obvious than that of AMT-GAN. Besides, the result shows that the detection of face forgery can not generalize to adv-faces although both deepfake faces and adv-faces are generated by GANs. This is possible because a huge difference exists between the fingerprints of deepfake GANs and that of adv-face GANs.

4.3 Ablation

Component ablation As argued, self-perturbation makes the detector learn a more generic representation of adv-faces, Max-Pooling Classifier captures abnormal local color aberrations, and the regularization term helps to boost adv-faces

Ablation	FGSM	DIM	TIM	TIP.	AdvM.	AMT.
w/o SP	100	92.5	72.4	66.1	52.1	50.8
w/o MPC	99.2	99.0	96.8	88.5	90.0	82.0
w/o LU	99.7	99.0	95.5	91.2	95.1	88.4
SP+MPC+LU	99.7	99.5	96.2	91.7	96.6	89.7

Table 5: AUC (%) comparison on CelebA-HQ dataset for ablation study. "w/o SP" means training on adv-faces generated by FGSM instead of self-perturbation. "MPC" refers to Max-Pooling Classifier. "LU" refers to training under the regularization $\mathcal{L}_{\text{uncertainty}}$. "AdvM." and "AMT." denote AdvMakeup and AMT-GAN respectively.

Self-Perturbation	FGSM	TIM	TIP.	AdvM.	AMT.
Point-wise	99.6	64.5	68.6	50.8	50.1
Block-wise	81.4	98.9	81.7	76.5	62.3
GC	65.5	70.7	68.0	85.5	78.0

Table 6: Detection AUC (%) on CelebA-HQ. Self-perturbed faces are generated using one of the self-perturbations. "GC" denotes self-perturbation for GAN-based attack mentioned in Algorithm 2.

detection. We then conduct an ablation study to verify the effectiveness of each component. As result shown in Table 5, detectors trained without self-perturbation totally failed in detecting adv-faces from TIPIM and GAN-based attacks, indicating the indispensability of self-perturbation in detecting advanced adversarial attacks. There is also an obvious gap between using and not using Max-Pooling Classifier, especially on GAN-based adv-faces. Narrowing the decision boundary, the regularization term helps to filter out a small number of adversarial samples which are not similar enough to self-perturbed faces, further improving detection performance. As for some gradient-based adv-faces such as DIM, detection accuracy is high enough regardless of using Max-Pooling Classifier and a regularization term. It is likely because self-perturbation is similar enough to attack noise patterns so that the representations learned by networks are generic enough.

Complementarity of self-perturbations To explore the necessity and complementarity of self-perturbations, we train a simple XceptionNet on self-perturbed faces generated from CelebA-HQ using only a single self-perturbation. The results are shown in Table 6. As we can see, training a detector only relying on one of the self-perturbations is insufficient for detecting all unseen adv-faces. Due to the differences in generation procedures, self-perturbations are complementary to each other in the detection tasks.

4.4 Analysis of Our Approach

Functionality of self-perturbations To explore the functionality of self-perturbations for gradient-based attacks, we extract noise features and face features of adversarial, self-perturbed, and real faces and visualize them using 2D t-SNE projection. As Figure 4 shows, self-perturbation is very close to attack noise and far from zero-vector (real faces). By separating real faces from self-perturbed faces, the trained network is able to distinguish between real and adv-faces indirectly. Although some adv-faces generated by TIM are not covered by self-perturbations, a model trained on decision boundary regularization still separates them from real faces.

ϵ	15	10	5	3	2	1
15	100	81.2	0.0	0.0	0.0	0.0
10	100	100	66.2	0.8	0.1	0.0
5	100	100	99.7	54.3	9.2	1.4
3	99.7	99.8	100	95.2	86.8	26.6
2	99.9	99.9	0.0	0.0	0.0	0.0
1	0.0	0.1	54.1	62.0	52.5	52.9

Table 7: Detection accuracy (%) on adv-faces generated by FGSM with various of perturbation magnitudes. Networks are trained on adv-faces at $\epsilon/255$ in the left column, and tested on adv-faces produced at $\epsilon/255$ in the top row.

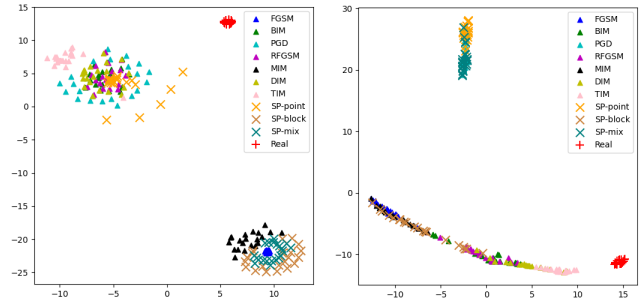


Figure 4: 2D t-SNE visualization. Left: flattened noise images of adv-faces and self-perturbed faces. 'SP-point' and 'SP-block' denotes point-wise and block-wise self-perturbations respectively, and 'SP-mix' means the mixture of the two perturbations. We use a zero-vector to represent the noise of real faces. Right: face features prior to the logit layer extracted by our model.

Impact of hyper-parameter Another experiment is about the choice of ϵ . We train a simple XceptionNet on FGSM adv-faces at $\epsilon = 1/255$ to $\epsilon = 15/255$ and test on adv-faces at different ϵ . As shown in Table 7, detectors trained on a smaller ϵ are able to detect adv-faces generated with a larger ϵ . But an extremely small ϵ may cause failure in model training. In practice, we do not need to select an extremely small value for ϵ because the attack success rate is too low to take into account as shown in the Appendix. In consideration of this, we choose $\epsilon = 5/255$ (attack success rate lower than 1%) for producing and detecting adv-faces.

5 Conclusion

In this paper, we investigate the intrinsic similarities of recent adv-faces and heuristically design three kinds of real face self-perturbations close to attack noise pattern. Regarding adv-faces as OOD data, we propose an FRS-agnostic and attack-agnostic cascaded system for adv-faces detection, which includes real face self-perturbations, decision boundary regularization, and Max-Pooling Classifier focusing on abnormal local color aberrations. Trained on only real faces and self-perturbed real faces, our model learned generic representations for adv-faces. Comprehensive analysis validates the proposed assumptions that noises of adv-faces have intrinsic similarities and exist in high-frequency areas, and extensive experiments demonstrate the improved effectiveness of our method compared with several recent baselines. Although our method achieves a satisfactory performance on detecting adv-faces (almost approaches saturation on LFW

dataset), we observe that the latent representation learned by the detector is hard to generalize to other domains. For instance, the detector trained on the LFW dataset fails to detect adv-faces generated from the CelebA-HQ dataset. For future work, we will try to solve this matter, by learning a more generic representation across various domains.

6 Acknowledgement

This work was supported in part by the Natural Science Foundation of China under Grant 61972169, in part by the National key research and development program of China(2019QY(Y)0202, 2022YFB2601802), in part by the Major Scientific and Technological Project of Hubei Province (2022BAA046, 2022BAA042), in part by the Research Programme on Applied Fundamentals and Frontier Technologies of Wuhan(2020010601012182) and the Knowledge Innovation Program of Wuhan-Basic Research, in part by China Postdoctoral Science Foundation 2022M711251.

References

- [Avarikioti *et al.*, 2019] Georgia Avarikioti, Kenan Basic, Yuyi Wang, and Roger Wattenhofer. Online payment network design, 2019.
- [Chollet, 2017] François Chollet. Xception: Deep learning with depthwise separable convolutions. In *2017 IEEE Conference on Computer Vision and Pattern Recognition (CVPR)*, pages 1800–1807, 2017.
- [Deng *et al.*, 2009] Jia Deng, Wei Dong, Richard Socher, Li-Jia Li, Kai Li, and Li Fei-Fei. Imagenet: A large-scale hierarchical image database. In *2009 IEEE Conference on Computer Vision and Pattern Recognition*, pages 248–255, 2009.
- [Deng *et al.*, 2019] Jiankang Deng, Jia Guo, Niannan Xue, and Stefanos Zafeiriou. Arcface: Additive angular margin loss for deep face recognition. In *2019 IEEE/CVF Conference on Computer Vision and Pattern Recognition (CVPR)*, pages 4685–4694, 2019.
- [Deng *et al.*, 2021] Zhijie Deng, Xiao Yang, Shizhen Xu, Hang Su, and Jun Zhu. Libre: A practical bayesian approach to adversarial detection. In *2021 IEEE/CVF Conference on Computer Vision and Pattern Recognition (CVPR)*, pages 972–982, 2021.
- [Dong *et al.*, 2018] Yinpeng Dong, Fangzhou Liao, Tianyu Pang, Hang Su, Jun Zhu, Xiaolin Hu, and Jianguo Li. Boosting adversarial attacks with momentum. In *2018 IEEE/CVF Conference on Computer Vision and Pattern Recognition*, pages 9185–9193, 2018.
- [Dong *et al.*, 2019] Yinpeng Dong, Tianyu Pang, Hang Su, and Jun Zhu. Evading defenses to transferable adversarial examples by translation-invariant attacks. In *2019 IEEE/CVF Conference on Computer Vision and Pattern Recognition (CVPR)*, pages 4307–4316, 2019.
- [Du *et al.*, 2022] Xuefeng Du, Zhaoning Wang, Mu Cai, and Yixuan Li. Vos: Learning what you don’t know by virtual outlier synthesis, 2022.
- [Duda and Hart, 1973] R. O. Duda and P. E. Hart. *Pattern Classification and Scene Analysis*. John Wiley & Sons, New York, 1973.
- [Dumbre *et al.*, 2016] Sudarshan Dumbre, Shamita Kulkarni, Devashree Deshpande, and P.V.Mulmule. Face detection and recognition for bank transaction. *Journal of emerging technologies and innovative research*, 3:108–112, 2016.
- [Feinman *et al.*, 2017] Reuben Feinman, Ryan R. Curtin, Saurabh Shintre, and Andrew B. Gardner. Detecting adversarial samples from artifacts, 2017.
- [Gary *et al.*, 2007] B. Huang Gary, Ramesh Manu, Berg Tamara, and Learned-Miller Erik. Labeled faces in the wild: A database for studying face recognition in unconstrained environments. Technical Report 07-49, University of Massachusetts, 2007.
- [Girish *et al.*, 2021] Sharath Girish, Saksham Suri, Saketh Rambhatla, and Abhinav Shrivastava. Towards discovery and attribution of open-world gan generated images. In *2021 IEEE/CVF International Conference on Computer Vision (ICCV)*, pages 14074–14083, 2021.
- [Goodfellow *et al.*, 2014] Ian J. Goodfellow, Jonathon Shlens, and Christian Szegedy. Explaining and harnessing adversarial examples, 2014.
- [He *et al.*, 2021] Yang He, Ning Yu, Margret Keuper, and Mario Fritz. Beyond the spectrum: Detecting deepfakes via re-synthesis. In *Proceedings of the Thirtieth International Joint Conference on Artificial Intelligence, IJCAI-21*, pages 2534–2541. International Joint Conferences on Artificial Intelligence Organization, 2021. Main Track.
- [Hsu *et al.*, 2020] Yen-Chang Hsu, Yilin Shen, Hongxia Jin, and Zsolt Kira. Generalized odin: Detecting out-of-distribution image without learning from out-of-distribution data. In *Proceedings of the IEEE/CVF Conference on Computer Vision and Pattern Recognition*, pages 10951–10960, 2020.
- [Hu *et al.*, 2022] Shengshan Hu, Xiaogeng Liu, Yechao Zhang, Minghui Li, Leo Yu Zhang, Hai Jin, and Libing Wu. Protecting facial privacy: Generating adversarial identity masks via style-robust makeup transfer. In *Proceedings of the IEEE/CVF Conference on Computer Vision and Pattern Recognition (CVPR)*, pages 15014–15023, 2022.
- [Karras *et al.*, 2017] Tero Karras, Timo Aila, Samuli Laine, and Jaakko Lehtinen. Progressive growing of gans for improved quality, stability, and variation, 2017.
- [Kim, 2020] Hoki Kim. Torchattacks: A pytorch repository for adversarial attacks, 2020.
- [Kurakin *et al.*, 2016] Alexey Kurakin, Ian Goodfellow, and Samy Bengio. Adversarial machine learning at scale, 2016.
- [Lee *et al.*, 2018] Kimin Lee, Kibok Lee, Honglak Lee, and Jinwoo Shin. A simple unified framework for detecting out-of-distribution samples and adversarial attacks.

- Advances in neural information processing systems*, 31, 2018.
- [Li *et al.*, 2020] Lixiang Li, Xiaohui Mu, Siying Li, and Haipeng Peng. A review of face recognition technology. *IEEE Access*, 8:139110–139120, 2020.
- [Liang *et al.*, 2017] Shiyu Liang, Yixuan Li, and R. Srikant. Enhancing the reliability of out-of-distribution image detection in neural networks, 2017.
- [Luo *et al.*, 2021] Yuchen Luo, Yong Zhang, Junchi Yan, and Wei Liu. Generalizing face forgery detection with high-frequency features. In *2021 IEEE/CVF Conference on Computer Vision and Pattern Recognition (CVPR)*, pages 16312–16321, 2021.
- [Ma *et al.*, 2018] Xingjun Ma, Bo Li, Yisen Wang, Sarah M. Erfani, Sudanthi Wijewickrema, Grant Schoenebeck, Dawn Song, Michael E. Houle, and James Bailey. Characterizing adversarial subspaces using local intrinsic dimensionality, 2018.
- [Madry *et al.*, 2017] Aleksander Madry, Aleksandar Makelov, Ludwig Schmidt, Dimitris Tsipras, and Adrian Vladu. Towards deep learning models resistant to adversarial attacks, 2017.
- [Ou *et al.*, 2017] Xinyu Ou, Hefei Ling, Han Yu, Ping Li, Fuhao Zou, and Si Liu. Adult image and video recognition by a deep multicontext network and fine-to-coarse strategy. *ACM Trans. Intell. Syst. Technol.*, 8(5), 2017.
- [Rössler *et al.*, 2019] Andreas Rössler, Davide Cozzolino, Luisa Verdoliva, Christian Riess, Justus Thies, and Matthias Niessner. Faceforensics++: Learning to detect manipulated facial images. In *2019 IEEE/CVF International Conference on Computer Vision (ICCV)*, pages 1–11, 2019.
- [Sagonas *et al.*, 2016] Christos Sagonas, Epameinondas Antonakos, Georgios Tzimiropoulos, Stefanos Zafeiriou, and Maja Pantic. 300 faces in-the-wild challenge: database and results. *Image and Vision Computing*, 47:3–18, 2016. 300-W, the First Automatic Facial Landmark Detection in-the-Wild Challenge.
- [Sharif *et al.*, 2016] Mahmood Sharif, Sruti Bhagavatula, Lujo Bauer, and Michael K Reiter. Accessorize to a crime: Real and stealthy attacks on state-of-the-art face recognition. In *Proceedings of the 2016 ACM SIGSAC conference on computer and communications security*, pages 1528–1540, 2016.
- [Shi *et al.*, 2020] Yuxuan Shi, Hefei Ling, Lei Wu, Jialie Shen, and Ping Li. Learning refined attribute-aligned network with attribute selection for person re-identification. *Neurocomputing*, 402:124–133, 2020.
- [Shiohara and Yamasaki, 2022] Kaede Shiohara and Toshiko Yamasaki. Detecting deepfakes with self-blended images, 2022.
- [Sun *et al.*, 2021] Yiyou Sun, Chuan Guo, and Yixuan Li. React: Out-of-distribution detection with rectified activations. *Advances in Neural Information Processing Systems*, 34:144–157, 2021.
- [Tian *et al.*, 2021] Jinyu Tian, Jiantao Zhou, Yuanman Li, and Jia Duan. Detecting adversarial examples from sensitivity inconsistency of spatial-transform domain. In *Proceedings of the AAAI Conference on Artificial Intelligence*, volume 35, pages 9877–9885, 2021.
- [Tong *et al.*, 2021] Liang Tong, Zhengzhang Chen, Jingchao Ni, Wei Cheng, Dongjin Song, Haifeng Chen, and Yevgeniy Vorobeychik. Facesec: A fine-grained robustness evaluation framework for face recognition systems. In *Proceedings of the IEEE/CVF Conference on Computer Vision and Pattern Recognition*, pages 13254–13263, 2021.
- [Tramèr *et al.*, 2018] Florian Tramèr, Alexey Kurakin, Nicolas Papernot, Ian Goodfellow, Dan Boneh, and Patrick McDaniel. Ensemble adversarial training: Attacks and defenses. In *International Conference on Learning Representations*, 2018.
- [Wei *et al.*, 2022] Hongxin Wei, Renchunzi Xie, Hao Cheng, Lei Feng, Bo An, and Yixuan Li. Mitigating neural network overconfidence with logit normalization. In *International Conference on Machine Learning*, pages 23631–23644. PMLR, 2022.
- [Wu *et al.*, 2021] Weibin Wu, Yuxin Su, Michael R. Lyu, and Irwin King. Improving the transferability of adversarial samples with adversarial transformations. In *2021 IEEE/CVF Conference on Computer Vision and Pattern Recognition (CVPR)*, pages 9020–9029, 2021.
- [Yang *et al.*, 2021] Xiao Yang, Yinpeng Dong, Tianyu Pang, Hang Su, Jun Zhu, Yuefeng Chen, and Hui Xue. Towards face encryption by generating adversarial identity masks. In *2021 IEEE/CVF International Conference on Computer Vision (ICCV)*, pages 3877–3887, 2021.
- [Yin *et al.*, 2021] Bangjie Yin, Wenxuan Wang, Taiping Yao, Junfeng Guo, Zelun Kong, Shouhong Ding, Jilin Li, and Cong Liu. Adv-makeup: A new imperceptible and transferable attack on face recognition. In *Proceedings of the Thirtieth International Joint Conference on Artificial Intelligence, IJCAI-21*, pages 1252–1258. International Joint Conferences on Artificial Intelligence Organization, 2021.
- [Yu *et al.*, 2019] Ning Yu, Larry Davis, and Mario Fritz. Attributing fake images to gans: Learning and analyzing gan fingerprints. In *2019 IEEE/CVF International Conference on Computer Vision (ICCV)*, pages 7555–7565, 2019.
- [Zhang and Sabuncu, 2018] Zhilu Zhang and Mert Sabuncu. Generalized cross entropy loss for training deep neural networks with noisy labels. In S. Bengio, H. Wallach, H. Larochelle, K. Grauman, N. Cesa-Bianchi, and R. Garnett, editors, *Advances in Neural Information Processing Systems*, volume 31. Curran Associates, Inc., 2018.
- [Zhang *et al.*, 2021] Baiyan Zhang, Hefei Ling, Jialie Shen, Qian Wang, Jie Lei, Yuxuan Shi, Lei Wu, and Ping Li. Mixture distribution graph network for few shot learning. *IEEE Transactions on Cognitive and Developmental Systems*, pages 1–1, 2021.

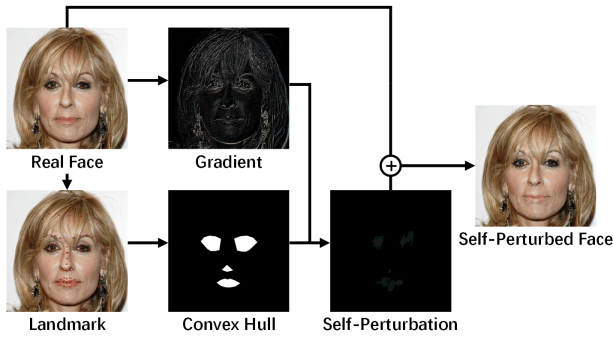


Figure 5: Pipeline of generating self-perturbations for GAN-based attack.

Appendix A Experimental details

In this section, we specify the procedure of real face self-perturbations including hyper-parameters, pipelines, and experiment equipment.

A.1 Implementation Details of Self-Perturbation

Real face self-perturbations are produced by using some random parameters. As for self-perturbations for the gradient-based attack, we use random noise value $\alpha \in [-5/255, 5/255]$ with perturbation magnitude $\epsilon = 5/255$.

For each self-perturbation for the gradient-based attack, mode is randomly selected where mode $\in \{\text{"point"}, \text{"block"}, \text{"mix"}\}$ and "mix" denotes the summation of "pixel" and "block" perturbations before clip operation. Noise patterns of gradient-based attack and self-perturbation are shown in Figure 8.

As for self-perturbations for GAN-based attacks, we set random perturbation magnitude to $\epsilon \in [10, 70]$. Real face images are sampled from the CelebA-HQ dataset with a size of 1024×1024 and then resized to 256×256 . A pixel from a convex hull is added to the high-frequency set H if its value is over a threshold of 50, and selected to the subset H_s by a probability in $[0.016, 0.040]$. Each gradient color (GC) patch is generated in a random size in $[2, 25] \times [2, 25]$. Before adding GC patches to high-frequency pixels, we randomly select a GC patch and add it to each pixel by a random probability of 0.8, and add other GC patches to the rest of the pixels. The high-frequency areas are the eyes, nose tip, and mouse. We portray the procedure of generating self-perturbations for GAN-based attack in Figure 5, and exhibit a set of them in Figure 9.

A.2 Software and Hardware

We run all experiments with Python 3.8.8 and PyTorch 1.10.0, using two NVIDIA GeForce RTX 1080 GPUs.

Appendix B Attack Success Rate

To better explain the reason why we use $\epsilon = 5/255$ in our experiments, we record the attack success rate (ASR) of FGSM, BIM, PGD, RFGSM, MIM, DIM, and TIM at different perturbation magnitude ϵ . Perturbation magnitude is set to $\epsilon \in \{5, 10, 15, 20\}$, the learning rate is set to $\alpha = 5$, and the amount of iteration steps is set to 10. The victim facial recognition system (FRS) is ArcFace. False Accept Rate

(FAR) for threshold selection is set to 0.01 and 0.001, and thresholds are computed as 27.25% and 31.99% respectively. Results are conducted on 7,484 adversarial faces (adv-faces) produced by attacking ArcFace. As shown in Tabel 8, ASR under $\epsilon = 5/255$ is a very small value to take into account, so we choose $\epsilon = 5/255$ for adv-faces detection evaluation.

All above ASR is calculated at $\alpha = 5$ and steps = 5. However, a smaller learning rate and larger steps may slightly promote the attack performance because a smaller learning rate will make attacks more sufficient especially when the perturbation is subtle. In view of this, all of adv-faces used in our main results are produced at $\alpha = 1$ and steps = 10.

Appendix C Validation of Intrinsic Similarities

Besides the FID metric reported in the main paper, we test the Learned Perceptual Image Patch Similarity (LPIPS) and draw a heat map to illustrate the similarities between various attacks. The heat map is shown in Figure 6.

Another quantitative method is about K-Means. We conduct a K-Means experiment on 7 gradient-based attacks at $K = 7$. If there is no similarity exists between these attacks, each attack would form a cluster and there is no intersection between the clusters. Otherwise, similarity exists. As shown in Table 9, noises from one attack always occur in two or more clusters, such as BIM contributes 26.9% to cluster 2, 45.5% to cluster 4, and 37.7% to cluster 5; RFGSM contributes 28.0% to cluster 2, 45.5% to cluster 4, and 36.8% to cluster 5. Clusters are visualized in Figure 7. It demonstrates the existing latent similarities that clusters always include noises from more than one attack.

Appendix D Detailed Ablation

In this section, we conduct ablation studies of classification mechanisms and regularization methods. The corresponding experiments of detecting GAN-made adv-faces on the CelebA-HQ dataset are shown in Table 10, which supports the improved effectiveness of our method. The analyses are as follows.

D.1 Classification Mechanism

Our Max-Pooling Classifier is designed to focus on local abnormal color variations which appear in GAN-made adv-faces. Once an anomaly appears somewhere, the entire image

ϵ	FAR	FGSM	BIM	PGD	RFGSM	MIM	DIM	TIM
5	0.01	0.03	0.05	0.11	0.15	0.41	0.84	0.09
	0.001	0.01	0.08	0.24	0.43	0.90	1.72	0.15
10	0.01	0.05	29.52	25.61	23.21	42.28	82.83	25.73
	0.001	0.08	38.05	34.01	31.63	50.25	87.44	34.09
15	0.01	0.25	44.00	35.26	59.07	70.22	96.85	65.11
	0.001	0.83	50.44	42.35	67.48	76.96	98.32	73.08
20	0.01	2.15	76.86	69.08	74.20	83.24	99.47	83.31
	0.001	5.17	83.03	76.76	81.81	88.03	99.80	88.54

Table 8: Attack success rate @FAR (%) of various of gradient-based adversarial attack methods at different $\epsilon/255$.

Cluster	FGSM	BIM	PGD	RFGSM	MIM	DIM	TIM
0			98.6				1.4
1	100						
2		26.9		28.0		45.1	
3							100
4		45.5		45.5		9.0	
5		37.7		36.8		25.5	
6					100		

Table 9: K-Means experimental result of adversarial attacks at $K = 7$. Each value indicates the proportion of an attack in a cluster.

Classifier	AdvM. AMT.		OOD	AdvM. AMT.	
Avg-Pooling	89.8	81.9	GODIN	72.0	79.5
Voting	87.5	80.4	LogitNorm	69.4	63.4
Max-Pooling	95.1	88.4	LU	90.0	82.0

Table 10: Ablation on classification strategies and OOD frameworks. The values indicate the detection AUC(%) using Xception-Net, the higher the better. The last row represents our optimal configuration. "LU" denotes our Decision Boundary Regularization. "AdvM." and "AMT." denote AdvMakeup and AMT-GAN respectively.

is considered an adv-face. We conduct an ablation study of the mechanism of the classifier compared with the average-pooling mechanism and voting mechanism. As shown in Table 10, max-pooling outperforms others because the average strategy would dilute the impact of local abnormal color variations, and a voting mechanism would backfire in case most regions are normal.

D.2 Regularization

Our Decision Boundary Regularization aims to shrink the decision boundary towards real faces so that adv-faces closed to the real are more likely to be detected. We compared our methods with training strategies of GODIN[Hsu et al., 2020] and LogitNorm[Wei et al., 2022], and it turns out more effective than other existing OOD frameworks.

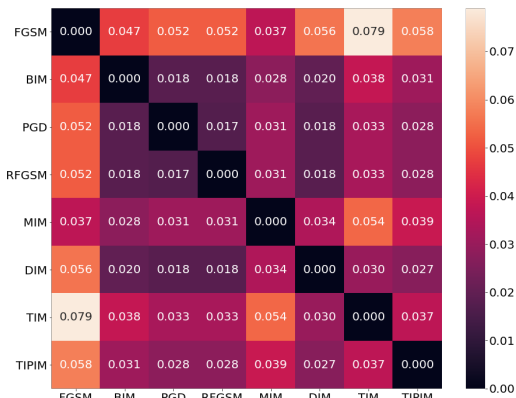


Figure 6: Learned Perceptual Image Patch Similarity (LPIPS) heat map of various attacks.

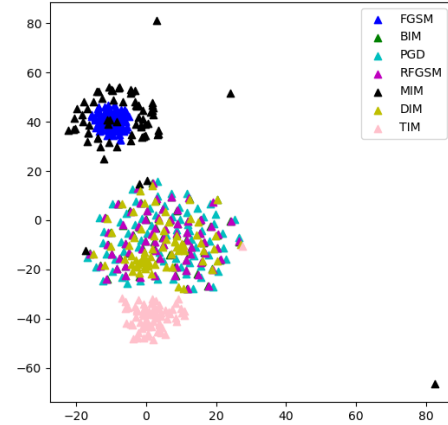


Figure 7: 2D t-SNE visualization of K-Means clusters.

Appendix E Facial Edition Attack and Natural Dataset

In this section, we test our methods against facial attribute attacks which are likely used in the physical world. We also test our methods by detecting adversarial examples from the general dataset to validate its independence from datasets.

E.1 Facial Attribute Attack Detection

We test our model by detecting three facial attribute editing attacks: sticker attack[Tong et al., 2021], eyeglass attack[Sharif et al., 2016], and face mask attack[Tong et al., 2021] on the VGGFace2 dataset. The results shown in Table 11 demonstrate the validity of our model.

Compared to GAN-based attacks, evidence of facial attribute editing attacks are easier to be detected since the editing traces are more obvious. Our hypotheses still hold for them because they also perturb high-frequency regions.

E.2 Experiment on General Dataset

We conduct experiments on CIFAR10 and ImageNet datasets, using only self-perturbation for the gradient-based attack. CIFAR10 is a general dataset with low resolution, while the resolution of ImageNet is higher. Consistent with the main paper, perturbation magnitude is set to $\epsilon = 5/255$ for both CIFAR10 and ImageNet. It is smaller than $\epsilon = 12.75/255$ used in baseline LID [Ma et al., 2018] for CIFAR10 and $\epsilon = 16/255$ used in LiBRE [Deng et al., 2021] for ImageNet, which means our setting is more challenging.

As shown in Table 12, our self-perturbation still works on general datasets with both lower and higher resolution. It shows that our method is domain-agnostic.

Method	Sticker[3]	Eyeglass[4]	Face Mask[3]
LID	51.0	64.7	53.2
SID	61.5	59.1	57.5
Ours	99.8	92.4	98.6

Table 11: AUC scores (%) of detecting facial editing attacks.

Dataset	FGSM	BIM	PGD	RF.	MIM	DIM	TIM
CIFAR10	99.8	99.7	99.8	99.8	99.6	99.8	94.4
ImageNet	99.3	98.6	98.8	98.6	98.3	99.3	98.3

Table 12: Detection AUC (%) on general image datasets.

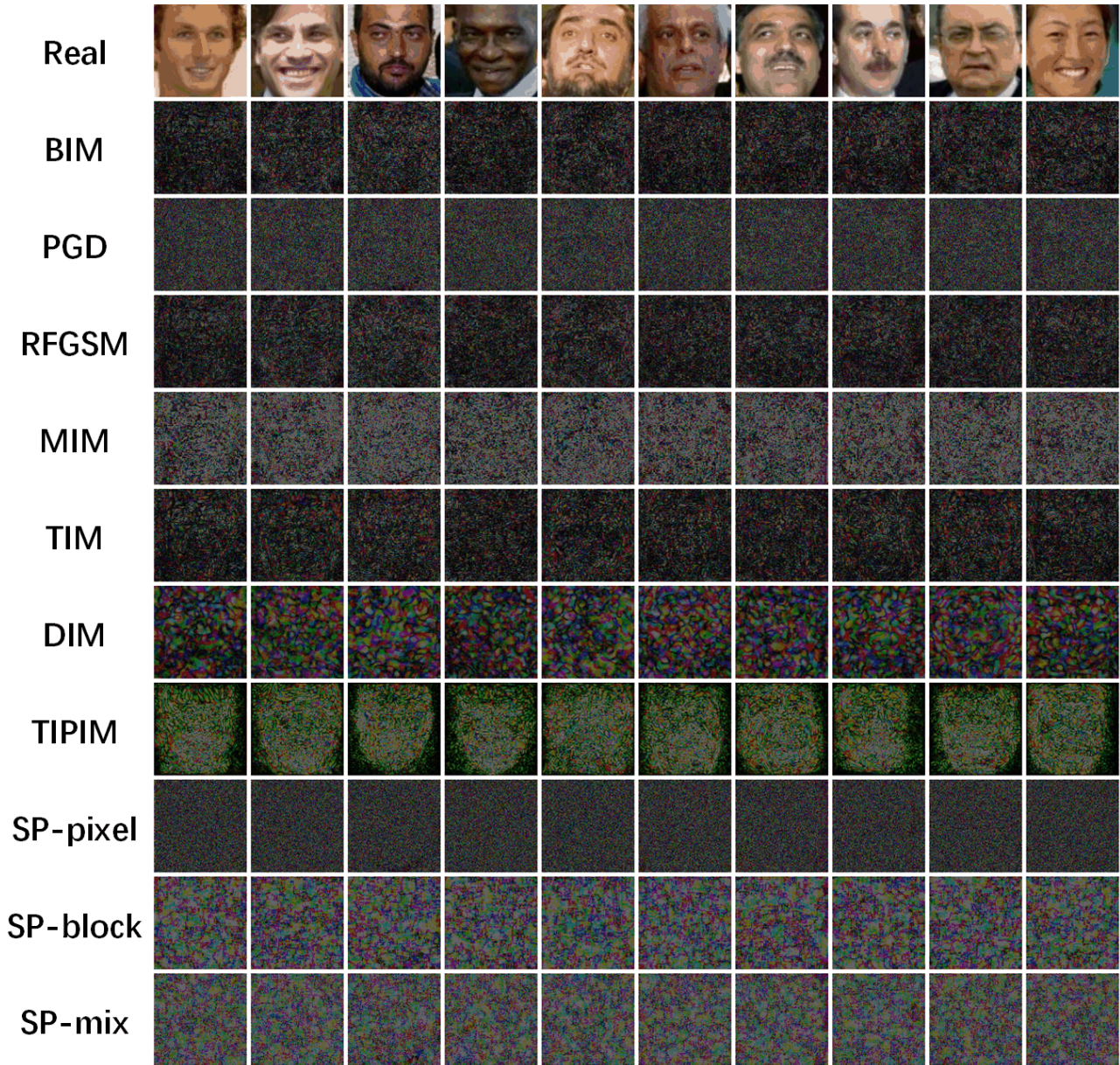


Figure 8: Noise images of gradient-based attacks and self-perturbations. All images are generated at $\epsilon = 10$. Values of noise images are 10 times expanded for better visualization.



Figure 9: Self-perturbed faces for GAN-based attacks. All real face images are sampled from the CelebA-HQ dataset.